Biosensors and Bioelectronics 25 (2010) 1875–1880

Contents lists available at ScienceDirect

Biosensors and Bioelectronics

journal homepage: www.elsevier.com/locate/bios

Reactive amine surfaces for biosensor applications, prepared by plasma-enhanced chemical vapour modification of polyolefin materials

C. Volcke[a,b,*,1], R.P. Gandhiraman[a,1], V. Gubala[a], J. Raj[c], Th. Cummins[a,d], G. Fonder[e], R.I. Nooney[a], Z. Mekhalif[e], G. Herzog[c], S. Daniels[a,f], D.W.M. Arrigan[c,2], A.A. Cafolla[a,d], D.E. Williams[a,g]

[a] Biomedical Diagnostics Institute, Dublin City University, Glasnevin, Dublin 9, Ireland
[b] Research Centre in Physics of Matter and Radiation, University of Namur (FUNDP), 61 rue de Bruxelles, 5000 Namur, Belgium
[c] Biomedical Diagnostics Institute Programme, Tyndall National Institute, University College Cork, Cork, Ireland
[d] School of Physical Sciences, Dublin City University, Glasnevin, Dublin 9, Ireland
[e] Laboratory of Chemistry and Electrochemistry of Surfaces, University of Namur (FUNDP), 61 rue de Bruxelles, 5000 Namur, Belgium
[f] National Center for Plasma Science and Technology, Dublin City University, Glasnevin, Dublin 9, Ireland
[g] MacDiarmid Institute for Advanced Materials and Nanotechnology, Department of Chemistry, University of Auckland, Private Bag 92019, Auckland 1142, New Zealand

ARTICLE INFO

Article history:
Received 21 October 2009
Received in revised form 8 December 2009
Accepted 29 December 2009
Available online 4 January 2010

Keywords:
Biosensors
Polymer
Plasma-enhanced chemical vapour deposition
Nanoparticle
DNA
Immunoassay

ABSTRACT

Here we have demonstrated a solventless plasma-based process that integrates low-cost, high throughput, high reproducibility and ecofriendly process for the functionalization of the next-generation point-of-care device platforms. Amine functionalities were deposited by plasma-enhanced chemical vapour deposition (PECVD) using a new precursor. The influence of the plasma RF power and the deposition time on surfacial properties, as well as their effect on the reactivity and content of amino groups was investigated. The key process determinants were to have a sufficient power in the plasma to activate and partially fragment the monomer but not too much as to lose the reactive amine functionality, and sufficient deposition time to develop a reactive layer but not to consume or erode the amine reactivity. An immunoassay performed using human immunoglobulin (IgG) as a model analyte showed an improvement of the detection limit by two orders of magnitude beyond that obtained using devices activated by liquid-phase reaction.

1. Introduction

Immobilization of biomolecules onto surfaces, and particularly onto polymeric substrates, is a key issue for the fabrication of next-generation biosensor devices. In this context, a new class of polymeric materials, Cyclo Olefin Polymers (COP), has received particular attention. Zeonor® is one such COP presenting excellent optical properties, good chemical resistance, ease of fabrication and cost effectiveness (Diaz-Quijada et al., 2007). These properties make Zeonor® particularly well-suited for sophisticated microchip designs including optical detection in biomedical and molecular diagnostic sensors.

Though several biomolecule immobilization techniques are reported in the literature, only a few recent communications address the issue of COP activation (Jönsson et al., 2008; Raj et al., 2009). In general, biomolecule immobilization is classified as chemical (Mateo-Martí et al., 2005) or physical (LaGraff and Chu-LaGraff, 2006). Chemical immobilization, through covalent linkage of biomolecules onto surfaces has shown good reproducibility and coverage, therefore becoming predominant. In such cases, liquid-phase deposition of functional groups, further attaching biomolecules, on activated surfaces is a routinely used procedure. For example, self-assembly of aminosilanes on oxidized silicon is one of the most studied methods (Song et al., 2008; Zhang and Srinivasan, 2004). These modification procedures are still not extensively investigated for polymers, for which physical immobilization is the dominant methodology.

Liquid-phase deposition of aminosilanes onto surfaces is demanding (water-free environment, time-consuming, hazardous materials) and hardly applicable to large industrial production requirements (Kurth and Bein, 1995). Oppositely, gas-phase deposition of amine-reactive groups, using plasma-enhanced chemical vapour deposition (PECVD) for example, overcomes the draw-

* Corresponding author at: Research Centre in Physics of Matter and Radiation, University of Namur (FUNDP), 61 rue de Bruxelles, 5000 Namur, Belgium. Tel.: +32 81 72 54 30; fax: +32 81 72 47 18.
E-mail address: cedric.volcke@fundp.ac.be (C. Volcke).
[1] These authors contributed equally.
[2] Current address: Nanochemistry Research Institute, Department of Chemistry, Curtin University of Technology, GPO Box U1987, Perth, WA 6845, Australia.

0956-5663/$ – see front matter © 2010 Elsevier B.V. All rights reserved.
doi:10.1016/j.bios.2009.12.034

backs of liquid-phase deposition (White and Tripp, 2000). PECVD has proven to be an excellent tool for surface modification at low temperatures (Dudek et al., 2009a; Gandhiraman et al., 2007; Muguruma and Kase, 2006). In principle, it offers significant advantages: uniformly diverse functional coating deposition on various surfaces; precise control of thickness; and adaptability for large mass production processing. Moreover, surface amination by PECVD was previously studied using, e.g., ethylene diamine (EDA) as precursor (Jung et al., 2006). Unfortunately, the adhesion and stability of these EDA films onto COP were very poor (unpublished data). The results were interpreted to imply merely physisorption and not reactive chemisorption of EDA molecules onto the polymeric surface.

New precursors, potentially presenting good adhesion and stability on polymeric surfaces, and also offering amine groups for subsequent reaction, are therefore needed. In this context, 3-(aminopropyl)triethoxysilane (APTES), commonly used for liquid-phase deposition (Qian et al., 1999; Simon et al., 2002) is expected to present all the requirements needed, expecting to result in reproducible silanized surfaces containing reactive amine groups, with good adhesion to COP through a siloxane network. COP substrates so functionalized could allow covalent attachment of a high surface density of active antibodies and DNA molecules, used as target molecules in biosensor devices, therefore lowering the limit of detection of the designed biosensor devices. The versatility, reproducibility and stability of this technique is expected to be applicable to a wide range of polymeric substrates for easy and rapid enhancement of actual (like ELISA) and future biosensors applications.

In this paper, we present a detailed investigation on the optimization of the reactive amine content of a deposited amino-film on a COP surface, for improved biomolecule attachment by appropriate choice of experimental parameters. Aminated coatings were prepared by PECVD of APTES onto a Zeonor® substrate. The influence of the plasma RF power and the deposition time on the deposited amount of amino functionalities and on their capacity for immobilizing nano-size objects (nanoparticles) and biomolecules (ssDNA) was investigated. Water contact angles (WCA), atomic force microscopy (AFM), ellipsometry and polarization modulation infrared reflection-absorption spectroscopy (PMIRRAS) were used for physical and chemical characterization. Fluorescence microscopy was performed to quantify the binding capacity of nanoparticles, amine-reactive fluorophore and labelled ssDNA molecules. An immunoassay was performed using human immunoglobulin G (IgG) as a model analyte.

2. Experimental part

2.1. Materials

Plain Zeonor® slides (Zeonor® 1060R) were obtained from Zeon Chemicals L.P. 3-aminopropyltriethoxysilane (APTES), Lissamine® rhodamine B sulfonyl chloride (λ_{exc} = 532 nm excitation and λ_{em} = 550 nm emission, further denominated as lissamine), acetonitrile, high purity HPLC grade water, glutaraldehyde, triethylamine, sodium dodecyl sulphate (SDS), pyridine, Tween 20®, dimethylformamide (DMF), 2-(*N*-morpholino)ethanesulfonic acid (MES) buffer, $MgCl_2$, methanol, phosphate buffered saline (PBS) solution, bovine serum albumin (BSA), the model analyte human IgG (IgG), capture antibody goat anti-human IgG (gαIgG) and Cy-5 labelled gαIgG were obtained from Sigma–Aldrich. ssDNA were obtained from MWG Biotech. 1-ethyl-3(3-dimethylaminopropyl)carbodiimide and *N*-hydroxysulfosuccinimide were purchased by Pierce. ABCR provided 1,4-phenyldithioisocyanate (PDITC).

2.2. PECVD system

The plasma deposition was carried out using a computer controlled Europlasma CD 300 PECVD system. The vacuum chamber was connected to a Dressler's CESAR 136 RF power source operating at 13.56 MHz, supplied with an automated impedance match-box for effective RF energy input to the plasma. The detailed description and a schematic of the system used is shown elsewhere (Dudek et al., 2009b; Gandhiraman et al., 2009).

2.3. Surface preparation

Dry air cleaned Zeonor® slides were introduced into the chamber before pumping down to a base pressure of 25 mTorr. APTES precursor stored in a heated container was connected to the chamber through a heated supply line (both at 80 °C). Plasma pretreatment was carried out using a mix of argon (50 sccm) and oxygen (50 sccm) plasma at 250 W RF power for 3 min. The oxygen supply was then closed and the plasma RF power decreased to the desired value. APTES was then introduced in the chamber for the required deposition time. The operating pressure was ~70 mTorr.

2.4. Surface characterization

2.4.1. Ellipsometry

The thickness of the APTES coatings on Zeonor® was characterized using J.A. Woollam Co., Inc EC-400, M-2000UI Spectroscopic Ellipsometer. All layers were modelled as a simple silicon dioxide dispersion layer to extract an effective thickness.

2.4.2. WCA

The film wettability was analyzed by measuring the water contact angle of the film surface (First 10 Å FTA200 contact angle analyser). High purity HPLC grade water was used.

2.4.3. Roughness measurements

AFM examinations were performed in ambient air with a commercial microscope (Dimension 3100 controlled by a Nanoscope IIIa controller, Digital Instruments), in the Tapping-Mode™, using standard silicon cantilevers (BudgetSensors®) with 42 N m^{-1} spring constant and a resonance frequency of about 300 kHz (nominal value). Topography was recorded at a scanning rate of 1–2 Hz. The surface roughness was evaluated over 3 AFM images (5 μm × 5 μm, Supporting Information) and the standard deviation then calculated. The root-mean-square roughness was defined as the average of height deviations taken from the mean plane (Haïdopoulos et al., 2007).

2.4.4. PMIRRAS

Substrates for PMIRRAS measurements were prepared following a procedure described elsewhere (Jönsson et al., 2008) (Supporting Information). PMIRRAS spectra were recorded on a Bruker Equinox 55-PMA37 spectra equipped with liquid nitrogen cooled mercury cadmium–telluride (MCT) detector and a zinc-selenide photoelastic modulator. The infrared light was modulated between s- and p-polarization at a frequency of 50 kHz. The incident angle upon the sample surface was around 85°. Signals generated from each polarization (R_s and R_p) were detected simultaneously by a lock-in amplifier and used to calculate the differential surface reflectivity $(\Delta R/R) = (R_p - R_s)/(R_p + R_s)$. The spectra were an average of 640 scans and were taken at a spectral resolution of 2 cm^{-1}.

2.4.5. Nanoparticle (NP) approach

Amino-functionalized silica NPs were prepared using a microemulsion method described previously (Arriagada and Osseo-Asare, 1999) (Supporting Information). The APTES coated

COP slides were dipped in an aqueous glutaraldehyde (2 wt%) solution for 24 h. Following this the slides were immersed in the amino-coated NPs solution (2.0 mg/ml) for a further 24 h, before intensive rinsing with DI water. After this, the NPs are covalently bound to coated COP surface. The NPs surface coverage was determined using AFM in conditions similar to roughness measurements. Nanoparticle counting was performed using the commercial Scanning Probe Image Processor program (SPIP™, Image Metrology).

2.4.6. Fluorescence

Fluorophore attachment to aminated COP substrates was achieved by immersing the samples for 1 h in a 0.23 mM lissamine in acetonitrile. 100 μl triethylamine was added to 100 ml of the lissamine solution. Samples were then rinsed with distilled water and sonicated for 5 min in a 0.1% SDS solution. Following, the substrates were rinsed again with distilled water and dried under a nitrogen stream. The fluorescence intensity was then measured using a plate scanner (GMS 418 scanner: Genetic Microsystems, Affymetrix). For the immobilization of fluorescently labelled DNA, slides were activated with PDITC linker by incubation of coated substrates for 3 h in a 5 mM solution of PDITC in anhydrous acetonitrile containing 1 wt% of pyridine. The slides were then washed three times in DMF and dried in a stream of nitrogen.

Afterwards, 50×10^{-7} M solution of the polynucleotide (5′-fluorescein labelled, 3′-C6 amino linker) was prepared by diluting the stock solution of ssDNA in 10 mM MES buffer containing 5 mM 1-ethyl-3(3-dimethylaminopropyl)carbodiimide, 10 mM $MgCl_2$ and 0.33 mM *N*-hydroxysulfosuccinimide. For post-processing, the slides were sonicated in 1% SDS for 5 min to remove the non-covalently bound ssDNA from the surface and then rinsed extensively with deionized water. The fluorescence intensity was then measured by the plate scanner.

2.5. Immunoassay

APTES modified slides were immersed in a 25 mM PDITC in DMF:pyridine (9:1 v/v) solution for 2 h, before rinsing with DMF and methanol and drying under a stream of nitrogen. For the immunoassay, 1 μl of the capture antibody, gαIgG (0.1 mg/ml) solution, at the desired concentration, was loaded on a PDITC-modified slide and incubated at 37 °C for 1 h. The surfaces were then washed with PBS containing Tween 20 (0.2% v/v) and further with PBS. The slides were subsequently immersed in a BSA (3% w/v) solution for 1 h. After rinsing with PBS, different concentrations of the model analyte IgG (0.02 pg/ml–0.2 mg/ml) were loaded (1 μl) and incubated at 37 °C for 1 h. The slides were washed with PBS, then the detection antibody Cy-5 labelled gαIgG (1 μl of 0.3 mg/ml) was printed using BioRobotics pins (1 μl) and incubated at 37 °C for 1 h. The device surfaces were subsequently washed with PBS containing Tween 20 (0.2%) solution twice, with PBS once and dried under a stream of nitrogen. The immunoassay was then ready for detection by measuring the fluorescence intensity Fluorescence images were acquired with an Olympus BX51 Epi-fluorescent microscope equipped with an Olympus DP71 Camera and appropriate filters. The excitation was obtained using an X-Cite Lamp Series 120 PC.

3. Results and discussion

PECVD deposited coatings were prepared under different conditions of RF plasma power at fixed deposition time (4 min), and of deposition time at fixed RF plasma power (14 W). We first present results obtained on coating deposited at fixed deposition time and further at fixed RF plasma power, followed by the selection of the one in each batch having the highest amount of amino groups. The surface reactivity was analyzed through nanoparticle, fluorophore and DNA attachment experiments. Finally immunoassay results are presented.

Table 1
Table presenting (1) the thickness; (2) the water contact angle and (3) the mean roughness of the PECVD deposited coating.

Deposition conditions	Layer thickness (nm)	Water contact angle (°)	Surface roughness R_{rms} (nm)
Zeonor®	–	92.2 ± 2.3	0.5 ± 0.1
4 min 7 W	9.0 ± 0.1	53.2 ± 1.4	1.4 ± 0.3
4 min 14 W	13.4 ± 0.3	60.6 ± 2.5	0.7 ± 0.1
4 min 25 W	19.2 ± 0.3	56.5 ± 1.1	1.2 ± 0.2
14 W 2 min	3.4 ± 0.1	55.4 ± 1.7	1.3 ± 0.1
14 W 4 min	13.4 ± 0.3	58.2 ± 1.4	0.7 ± 0.1
14 W 8 min	17.2 ± 0.3	60.0 ± 1.0	0.9 ± 0.1

3.1. At fixed deposition time of 4 min

For coatings obtained at 7 W, 14 W and 25 W RF power after 4 min deposition, the layer thickness, WCA and surface roughness values are presented in Table 1. Although variations highlighted in Table 1 are relatively small, the thickness clearly increased, at first steeply, and then more gradually, with increasing plasma RF power. These values are consistent with the formation of a thick layer, and not a monolayer. Although the species present in the plasma are not known in detail, the coating formation can reasonably be explained as follows: the decomposition of the monomer (APTES) into fragments is induced by the plasma; these fragments then deposit and covalently bind to the activated surface and to each other to form a fairly non-organized thick coating (Supporting Information). Plasma electron density measurements using a hair pin probe (Supporting Information) show that electron density (and hence plasma density) increased with increasing RF plasma power. The increased deposited thickness can therefore be explained as a consequence of the enhanced decomposition of the reactants induced by an increase in the plasma density, as previously reported for similar systems (Kulisch et al., 1989).

The equilibrium WCA highlight similar values for the three surfaces: around 55–60°. Thus, after coating deposition, the surfaces are more hydrophilic compared to plain COP (~92°), as expected. Moreover, the three coatings had similar hydrophilicity, independently of the plasma power used and is similar to literature values for liquid-phase deposited APTES molecules on silicon oxide surfaces (Cho and Ivanisevic, 2004). All coatings were also very smooth (roughness values between 0.7 and 1.4 nm, Table 1). A uniform deposition over the polymeric surface, independently of the plasma power condition used, therefore occurred. It is noteworthy that roughness modifications due to uncontrolled aminosilane polymerization on the surface were not present here, illustrating one advantage of the PECVD deposition process.

The coatings PMIRRAS spectra (Fig. 1) contain several vibrational features (missing on uncoated substrate spectrum) associated to bulk content of the deposited aminosilane coating, the most prominent being located in the 1300–1000 cm^{-1}, 1800–1500 cm^{-1} and 3500–3200 cm^{-1} regions (Fig. 1; Region 1, 2 and 3 respectively).

Bands in Region 1 have three main components located at 1265 cm^{-1}, 1220 cm^{-1} and 1199 cm^{-1}. These are assigned to symmetric deformation of Si–CH_3 (1265 cm^{-1}), Si–CH_2-R deformation (1220 cm^{-1}), and Si–O–C and C–N vibrations (1199 cm^{-1}) (Socrates, 2004; Wavhal et al., 2006). Some variations in the IR absorption peak intensities are also observed. We can reasonably assume an isotropic orientation of the deposited molecules in the coating and an independency of the orientation of the (fragmented) molecules with the deposition conditions used, so that IR peak intensities can be correlated to the amount of molecules/functional groups in the surface and the bulk of the coating, without taking into account

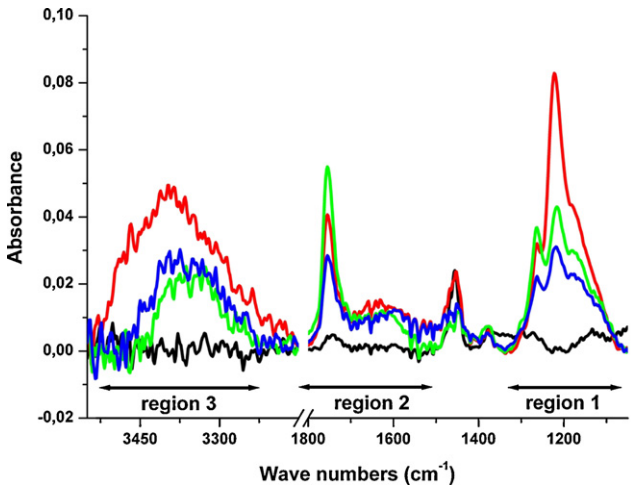

Fig. 1. PMIRRAS spectra of bare COP surfaces (black) and PECVD coating on COP surfaces deposited at fixed deposition time (4 min) and varying RF plasma power of 7 W (red), 14 W (green) and 25 W (blue). Three region of interest are highlighted: 1300–1000 cm^{-1} (region 1), 1800–1500 cm^{-1} (region 2) and 3500–3200 cm^{-1} (region 3).

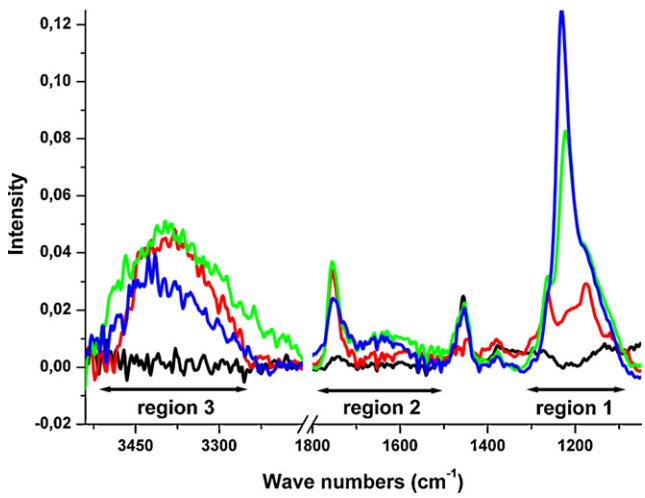

Fig. 2. PMIRRAS spectra of bare COP surfaces (black) and PECVD coating on COP surfaces deposited at fixed RF plasma power (14 W) and varying deposition time of 2 min (red), 4 min (green) and 8 min (blue). Three region of interest are highlighted: 1300–1000 cm^{-1} (region 1), 1800–1500 cm^{-1} (region 2) and 3500–3200 cm^{-1} (region 3).

orientation effects. The analysis of the peak intensities in Region 1 revealed that peaks were generally more intense for the 7 W coating, with a decreasing tendency in peak intensities as the RF plasma power increases. Thus, although the deposited layer thickness increased with increasing power, the silicon content of the layer decreased.

In Region 2 (Fig. 1), the presence of carboxylic group vibrational peaks (at 1754 cm^{-1} and 1734 cm^{-1} associated to ν(C=O) ester and ν(C=O) carboxylic acid) was observed (Dreesen et al., 2007) and their intensity varied following the trend:

$$I(C{=}O)_{25\,W} < I(C{=}O)_{7\,W} < I(C{=}O)_{14\,W}$$

Oxygenated surface species could originate from the initial surface treatment but pre-treatment conditions were identical for all coatings, which should not affect the C=O peak intensity. Therefore, this trend is related to dissociation of the silane producing ethoxy radicals. The observed intensity variations could arise from reactions with radicals from APTES monomer of the carboxylic groups formed in the initial surface activation, as previously deduced by others using different monomers under similar conditions (Bae et al., 2007). As the radicals created in the plasma differ according to plasma power conditions, they would react differently with the surface and a variable C=O vibration intensity is thus expected. Carboxyl functions could also be built through rearrangement and fragmentation of ethoxy radicals. Such processes could account for the variation of carboxylate concentration in the films at the highest power.

Vibrations associated with primary NH_2 vibrations are also identified in the 1650–1600 cm^{-1} range (Region 2, Fig. 1). With increasing RF plasma power, this amine peak was slightly shifted towards lower wavenumbers, indicative of the transformation of free amines into hydrogen-bonded amines (Kanan et al., 2002). A broad band associated to the presence of primary amines was also observed on all coatings in the range 3500–3200 cm^{-1} (Region 3, Fig. 1). The NH_2 vibration intensity in both Region 2 and 3 were highest in the 7 W coating spectrum. The decrease in the NH_2 IR absorption bands with increase in the RF plasma power implies a decrease in the amine content of the coatings. The results indicate that, at the lowest power, the silane was activated and could react with the surface, but was not significantly dissociated. With increasing power, the silane became fragmented, with amine functions being lost and the layer being built through reaction of ethoxy radicals.

3.2. At fixed power

At fixed plasma power (14 W), as the deposition time increased, the coating thickness also increased (Table 1). Again, the measured values are consistent with the formation of a non-organized thick multilayer. The WCA values (Table 1) showed that the hydrophilicity varied from ~92° for plain COP to ~60° after coating deposition, as expected. However, it was similar amongst the coatings considered. Moreover, all coatings were very smooth (roughness values between 0.7 and 1.3 nm, Table 1). Values were similar for all conditions, including plasma power variation, indicating the invariance of the roughness with the deposition condition.

Fig. 2 highlight changes in the PMIRRAS spectra of the bulk and surface of the coating with varying deposition time. All peaks in the 1100–1300 cm^{-1} region (Region 1, Fig. 2) associated with silane vibration increased with increasing deposition time. The peak centred around 1200–1170 cm^{-1} (Si–O–C rocking and C–N vibrations) and around 1230–1210 cm^{-1} (Si–CH_2-R vibration) increased slightly in wavenumber with increasing deposition time (Socrates, 2004). The peak intensities associated with amine and carboxylate functions, at around 1700 cm^{-1} (Region 2, Fig. 2) and 3200–3500 cm^{-1} (Region 3, Fig. 2) followed the trend:

$$[NH_2, C{=}O]_{8\,min} < [NH_2, C{=}O]_{2\,min} < [NH_2, C{=}O]_{4\,min}$$

There were also changes in peak position in the amine region (Region 2, Fig. 2). The 2 min, 4 min and 8 min coating presented a peak centred at 1594 cm^{-1}, at 1624 cm^{-1} and at 1644 cm^{-1}, respectively, indicative of an increase in the hydrogen-bonded character of the amino groups (Kanan et al., 2002).

As deposition time increased, the thickness of the deposited layer increased. However, for deposition times longer than 4 min, the ester and amine amount decreased with increasing deposition time. We rationalize this by the fact that, during the plasma deposition, the growing film surface is exposed to the plasma. Therefore, as the plasma exposure time is increased, the reactive groups on the growing film surface, including amines and esters, might undergo functional changes induced by plasma generated species such as ions and charged radicals (Kim et al., 2003). The maximum peak intensity assigned to amines was observed at deposition time of

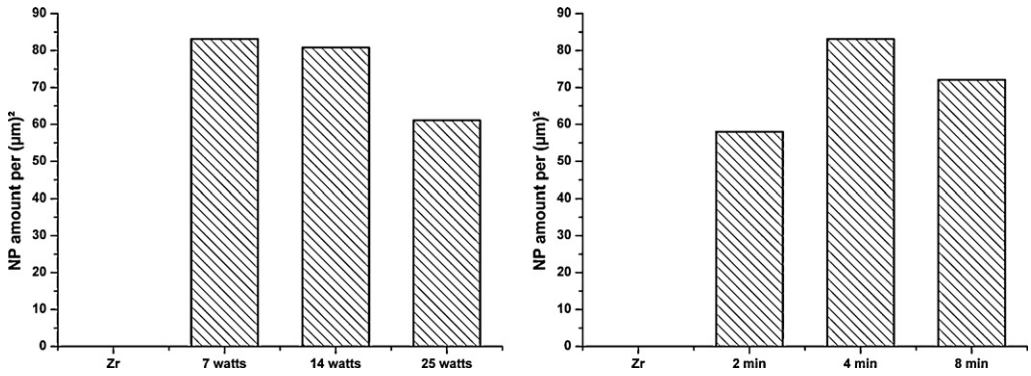

Fig. 3. Graphical representation of the number of nanoparticles attached per micron square on coated COP surfaces at fixed deposition time (left) and fixed RF plasma power (right).

4 min. This appeared to be the optimal condition at which a reasonable mass of amines could be formed on the surface. Longer exposure to the plasma seemed to trigger structural changes of the functional groups of interest.

3.3. Reactivity and binding capacity

In the nanoparticle approach, a homo-bifunctional cross-linker, glutaraldehyde, was used to covalently attach the amino-functionalized silica NP to the coated COP surface. The nanoparticle density/distribution was then imaged using AFM (Supporting Information). Fig. 3 shows the NPs amount per micron square on all coatings. As expected, the uncoated Zeonor® surface was unreactive. At fixed deposition time (4 min), the bounded NPs number was very similar for plasma powered at 7 and 14 W. Then, it declined with increase of power to 25 W. At fixed RF power (14 W), the attached NPs number increased to a maximum value with increasing deposition time. So, coatings presenting the highest amount of free NH_2 (as indicated by PMIRRAS spectroscopy) attached the highest NPs amount. In other words, larger amine content resulted in better NP attachment capacity. Although the nanoparticle distribution cannot directly reveal the amount of amine groups on the surface, it can provide an idea of their density, distribution and their capability to bind nano-objects. However, this nanoparticle approach has some limitations mainly due to surface saturation, which makes the method dependent on NP size, for example. Moreover, the coating stability and presence after washing steps is confirmed through those experiments as NPs are still observed at the end of the process. The results are consistent with our hypothesis that APTES fragments formed in the plasma covalently bond onto the COP surface upon deposition, which is not the case for EDA fragments. The presence of Si–O– groups apparently plays an important role in the formation of chemisorbed amino coatings onto activated polymeric substrates.

To further investigate the reactivity of preselected coatings (14 W–4 min and 7 W–4 min), the coupling reaction of aminated surfaces to an amine-reactive fluorophore was studied. Fig. 4 shows on the 14 W–4 min coating double intensity that on the 7 W–4 min coating, indicating the presence of twice the amount of reactive surfacial amino groups, if we assume one fluorophore per surfacial amino group. Although both selected coatings presented similar NP attachment, they behaved significantly differently while attaching fluorophores. This is probably due to size effects: the nanoparticles used were ~60 nm in diameter; the fluorophore has a size in the nanometre range.

To demonstrate biomolecule binding capacity, DNA attachment was performed. Fluorescence intensities measured after attachment of a polynucleotide (Fig. 4) indicated the 14 W coated surface to be three times more performant in attaching DNA molecules than the 7 W coated one. However, the PMIRRAS NH_2 peak area was twice larger in the 7 W deposited films than in the 14 W film. This indicates that, whilst there could have been more amines in the 7 W coating than in the 14 W, either they were not present at the surface or they were not reactive. It seems unlikely that the

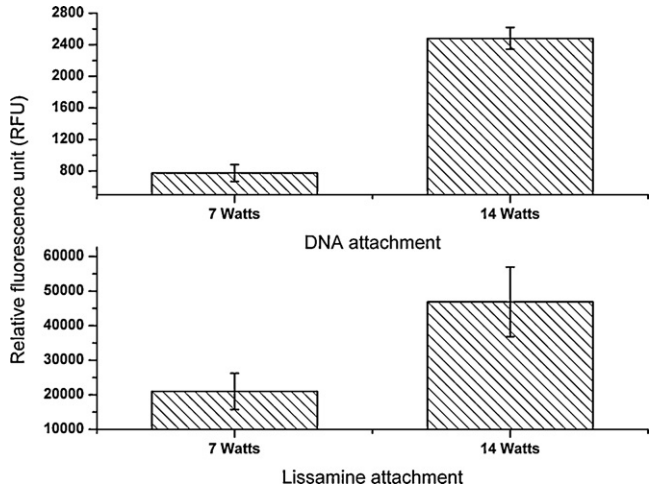

Fig. 4. Fluorescence intensity measured after fluorophore (bottom) and DNA attachment (top) on the 7 W–4 min and 14 W–4 min coatings.

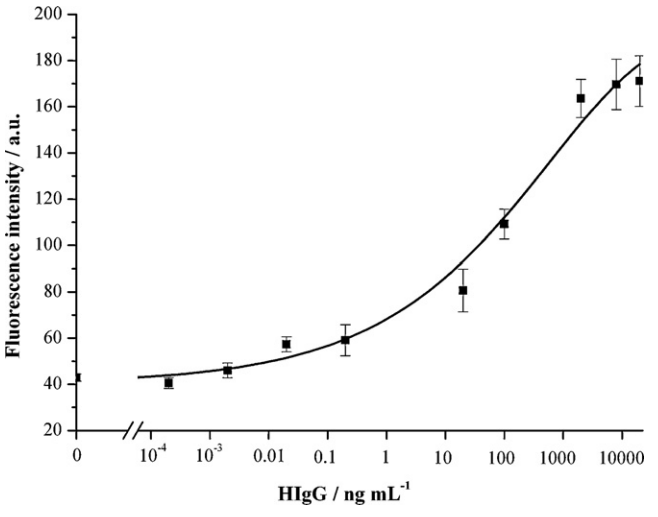

Fig. 5. Fluorescence linked immunosorbent assays for the detection of IgG as the model analyte.

coating varied significantly in its composition through its thickness. We deduced earlier that one effect of increasing the plasma power was to increase fragmentation of the silane. Thus, we speculate that, in the layer formed with 7 W power, the formation of a layer from largely intact silane also resulted in a network that bonded and constrained the amine groups within the interior of the layer. Fragmentation of the silane could produce ethoxy and alkyl amino radicals. One hypothesis is that insertion of alkyl amino radicals into the network at the surface of the growing film was responsible for creating the higher amount of surface reactive amines present in the film formed with a higher power.

The applicability of such coatings for biosensor platforms was demonstrated through an antibody/antigen bioassay, Fig. 5. The 14 W–4 min APTES coated slide was employed in a typical sandwich immunoassay format using gαIgG and Cy5-labeled gαIgG as capture and detection antibodies respectively, and IgG as the model analyte. The limit of detection (corresponding to the background signal plus three times the standard deviation of the background signal) was determined to be 5.7 pg ml^{-1}. This value is two orders of magnitude better than the ones obtained with immunosensors modified by silanization in solution (Boozer et al., 2006; Vikholm-Lundin and Albers, 2006). Further, such APTES coated COP slides are stable over time as contact angle values are fairly stable even after 5 week while stored in air (unpublished data), increasing the future range of applications of such platform.

4. Conclusions

Cyclo Olefin Polymer surfaces were successfully functionalized through the PECVD deposition of a new precursor, APTES, yielding amine functional groups available for biomolecule attachment. The deposition conditions were optimized in order to gain the most performant surface in attaching nanoparticles and DNA molecules. We identified the effect of plasma power in both activating and fragmenting the silane, and in both building the layer and eroding it. The consequences were that, in our system, whilst the thickness of the layer could be increased by increasing power and deposition time, the chemical functionality was optimal at a specific combination of parameters. We speculated that the effect of fragmentation of the silane into siloxane, ethoxy and alkyl amine radicals was the determining factor. An immunoassay performed using human IgG as a model analyte shows an improvement of the detection limit by two orders of magnitude beyond that obtained using devices activated by liquid-phase reaction.

Acknowledgements

This material is based upon works supported by the Science Foundation Ireland (S.F.I.) under Grant No. 05/CE3/B754. D.E.W. is an E.T.S. Walton Visiting Fellow of Science Foundation Ireland. C.V. is a postdoctoral researcher of the Belgian Fund for Scientific Research (F.R.S./F.N.R.S.).

Appendix A. Supplementary data

Supplementary data associated with this article can be found, in the online version, at doi:10.1016/j.bios.2009.12.034.

References

Arriagada, F.J., Osseo-Asare, K., 1999. J. Colloids Interface Sci. 211, 210–220.
Bae, I.-S., Jung, C.K., Cho, S.-J., Song, Y.-H., Boo, J.H., 2007. J. Korean Phys. Soc. 50, 1854–1857.
Boozer, C., Ladd, J., Chen, S., Jiang, S., 2006. Anal. Chem. 78, 1515–1519.
Cho, Y., Ivanisevic, A., 2004. J. Phys. Chem. B 108, 15223–15228.
Diaz-Quijada, G.A., Peytavi, R., Nantel, A., Roy, E., Bergeron, M.G., Dumoulin, M.M., Veres, T., 2007. Lab Chip 7, 856–862.
Dudek, M.M., Gandhiraman, R.P., Volcke, C., Cafolla, A.A., Daniels, S., Killard, A.J., 2009a. Langmuir 25, 11155–11161.
Dudek, M.M., Gandhiraman, R.P., Volcke, C., Daniels, S., Killard, A.J., 2009b. Plasma Process. Polym. 6, 620–630.
Dreesen, L., Silien, C., Volcke, C., Sartenaer, Y., Thiry, P.A., Peremans, A., Grugier, J., Marchand-Brynaert, J., Brans, A., Grubisic, S., Joris, B., 2007. Chem. Phys. Chem. 8, 1071–1076.
Haïdopoulos, M., Mirabella, F., Horgnies, M., Volcke, C., Thiry, P.A., Rouxhet, P., Pireaux, J.J., 2007. J. Microsc. 228, 227–239.
Gandhiraman, R.P., Daniels, S., Cameron, D.C., 2007. Plasma Process Polym. 4, S369–S373.
Gandhiraman, R.P., Karkari, S.K., Daniels, S., MacCraith, B.D., 2009. Surf. Coat. Technol. 203, 3521–3526.
Jönsson, C., Aronsson, M., Rundström, G., Pettersson, C., Mendel-Hartvig, B., Bakker, J., Martinsson, E., Liedberg, B., MacCraith, B.D., Öhman, O., Melin, J., 2008. Lab Chip 8, 1191–1197.
Jung, D., Yeo, S., Kim, J., Kim, B., Jin, B., Ryu, D.-Y., 2006. Surf. Coat. Technol. 200, 2886–2891.
Kanan, S.M., Tze, W.T.Y., Tripp, C.P., 2002. Langmuir 18, 6623–6627.
Kim, J., Park, H., Jung, D., Kim, S., 2003. Anal. Biochem. 313, 41–45.
Kulisch, W., Lippmann, T., Kassing, R., 1989. Thin Solid Films 174, 57–61.
Kurth, D.G., Bein, T., 1995. Langmuir 11, 3061–3067.
LaGraff, J.R., Chu-LaGraff, Q., 2006. Langmuir 22, 4685–4693.
Mateo-Martí, E., Briones, C., Román, E., Briand, E., Pradier, C.M., Martín-Gago, J.A., 2005. Langmuir 21, 9510–9517.
Muguruma, H., Kase, Y., 2006. Biosens. Bioelectron. 22, 737–743.
Qian, W., Yao, D., Xu, B., Yu, F., Lu, Z., Knoll, W., 1999. Chem. Mater. 11, 1399–1401.
Raj, J., Herzog, G., Manning, M., Volcke, C., McCraith, B.D., Ballantyne, S., Thompson, M., Arrigan, D.W.M., 2009. Biosens. Bioelectron. 24, 2654–2658.
Simon, A., Cohen-Bouhacina, T., Porté, M.C., Aimé, J.P., Baquey, C., 2002. J. Colloid Interface Sci. 251, 278–283.
Socrates, G., 2004. Infrared and Raman Characteristic Group Frequencies. Wiley VCH, Chichester.
Song, S., Zhou, J., Qu, M., Yang, S., Zhang, J., 2008. Langmuir 24, 105–109.
Vikholm-Lundin, I., Albers, W., 2006. Biosens. Bioelectron. 21, 1141–1148.
Wavhal, D.S., Zhang, J., Steen, M.L., Fisher, E.R., 2006. Plasma Process. Polym. 3, 276–287.
White, L.D., Tripp, C.P., 2000. J. Colloid Interface Sci. 232, 400–407.
Zhang, F., Srinivasan, M.P., 2004. Langmuir 20, 2309–2314.